

THE SPITZER SPACE TELESCOPE MISSION

M. W. WERNER,¹ T. L. ROELLIG,² F. J. LOW,³ G. H. RIEKE,³ M. RIEKE,³ W. F. HOFFMANN,³ E. YOUNG,³ J. R. HOUCK,⁴
B. BRANDL,⁵ G. G. FAZIO,⁶ J. L. HORA,⁶ R. D. GEHRZ,⁷ G. HELOU,⁸ B. T. SOIFER,⁸ J. STAUFFER,⁸ J. KEENE,^{8,9}
P. EISENHARDT,⁹ D. GALLAGHER,⁹ T. N. GAUTIER,⁹ W. IRACE,⁹ C. R. LAWRENCE,⁹ L. SIMMONS,⁹
J. E. VAN CLEVE,¹⁰ M. JURA,¹¹ E. L. WRIGHT,¹¹ AND D. P. CRUIKSHANK²

Received 2004 March 26; accepted 2004 May 26

ABSTRACT

The *Spitzer Space Telescope*, NASA's Great Observatory for infrared astronomy, was launched 2003 August 25 and is returning excellent scientific data from its Earth-trailing solar orbit. *Spitzer* combines the intrinsic sensitivity achievable with a cryogenic telescope in space with the great imaging and spectroscopic power of modern detector arrays to provide the user community with huge gains in capability for exploration of the cosmos in the infrared. The observatory systems are largely performing as expected, and the projected cryogenic lifetime is in excess of 5 years. This paper summarizes the on-orbit scientific, technical, and operational performance of *Spitzer*. Subsequent papers in this special issue describe the *Spitzer* instruments in detail and highlight many of the exciting scientific results obtained during the first 6 months of the *Spitzer* mission.

Subject headings: space vehicles: instruments — telescopes

1. INTRODUCTION

The *Spitzer Space Telescope*, NASA's Great Observatory for infrared astronomy, was launched 2003 August 25 and is performing extremely well, returning excellent scientific data from its Earth-trailing solar orbit. *Spitzer* incorporates an 85 cm diameter telescope primary mirror, cooled to as low as 5.5 K, and three scientific instruments providing imaging and spectroscopy at wavelengths from 3.6 to 160 μm . The observatory systems are largely performing as expected, and the projected cryogenic lifetime is in excess of 5 years. The ground systems and operations teams at the Jet Propulsion Laboratory, Lockheed Martin Astronautics, and the *Spitzer* Science Center are routinely downloading 1.1 Gbytes of data per day and delivering the pipeline-processed science data to the observer within 14 days. This paper provides an overview of the observatory design and performance, emphasizing the pointing, optical, and cryothermal systems that are of immediate concern to the *Spitzer* user community. We also present summaries of the instrumental capabilities and sensitivities, and of the orbit and operations. The results presented in companion papers in this special issue show that *Spitzer* will provide both greatly increased understanding of known astrophysical questions and discoveries that define new areas of scientific inquiry. At the same time, *Spitzer* demonstrates a number of observatory and mission design

innovations that can be productively incorporated into future space programs. Current details on *Spitzer* status and performance can be found on the *Spitzer* Science Center Web site.¹²

2. SATELLITE DESIGN

The *Spitzer* flight hardware consists of a spacecraft that operates at roughly ambient temperature and a cryogenic telescope assembly (CTA) that is cooled by a combination of superfluid liquid helium, helium boil-off gas, and radiative cooling and operates at much lower temperatures. The spacecraft was built by Lockheed Martin, Sunnyvale, California, and the CTA by Ball Aerospace. The two components are thermally isolated from each other by a system of low-thermal-conductivity struts and shields. The overall layout of the flight configuration is shown in Figure 1, and a summary of information about the complete flight system is given in Table 1. More detailed descriptions of the two components are given below.

The Spacecraft.—The *Spitzer* spacecraft handles the observatory's power generation, pointing and momentum control, data processing and storage, and telecommunications functions. It also contains the warm electronics portions of the three scientific instruments. The spacecraft structure itself is octagonally shaped, constructed from graphite composite and aluminum honeycomb material, and is mounted to the cold CTA with low thermal conductivity gamma-alumina struts. A set of aluminized Mylar thermal blankets and aluminum/graphite epoxy honeycomb radiation shields dramatically reduces the radiative thermal load from the warm spacecraft onto the CTA. A similar system of thermal shields attenuates the thermal radiation from the solar array, which is cantilevered from the spacecraft structure without any physical connection to the cold CTA. There are approximately 1500 wires that run from the warm spacecraft to the cold CTA. These were constructed of very low thermal conductivity materials and carefully heat-sunk so that they caused minimal parasitic heat input. The spacecraft avionics are fully redundant, as are the components of the pointing and control system (PCS) and reaction control system (RCS) discussed below.

¹ Jet Propulsion Laboratory, MS 264-767, 4800 Oak Grove Drive, Pasadena, CA 91109; mwerner@sirtfweb.jpl.nasa.gov.

² NASA Ames Research Center, MS 245-6, Moffett Field, CA 94035-1000.

³ Steward Observatory, University of Arizona, 933 North Cherry Avenue, Tucson, AZ 85721.

⁴ Astronomy Department, Cornell University, Ithaca, NY 14853-6801.

⁵ Leiden University, 2300 RA Leiden, Netherlands.

⁶ Harvard-Smithsonian Center for Astrophysics, 60 Garden Street, Cambridge, MA 02138.

⁷ Department of Astronomy, School of Physics and Astronomy, 116 Church Street SE, University of Minnesota, Minneapolis, MN 55455.

⁸ *Spitzer* Science Center, California Institute of Technology, Pasadena, CA 91125.

⁹ Jet Propulsion Laboratory, 4800 Oak Grove Drive, Pasadena, CA 91109.

¹⁰ Ball Aerospace and Technologies, 1600 Commerce Street, Boulder, CO 80301.

¹¹ Department of Physics and Astronomy, University of California, Los Angeles, CA 90095-1562.

¹² At <http://ssc.spitzer.caltech.edu>.

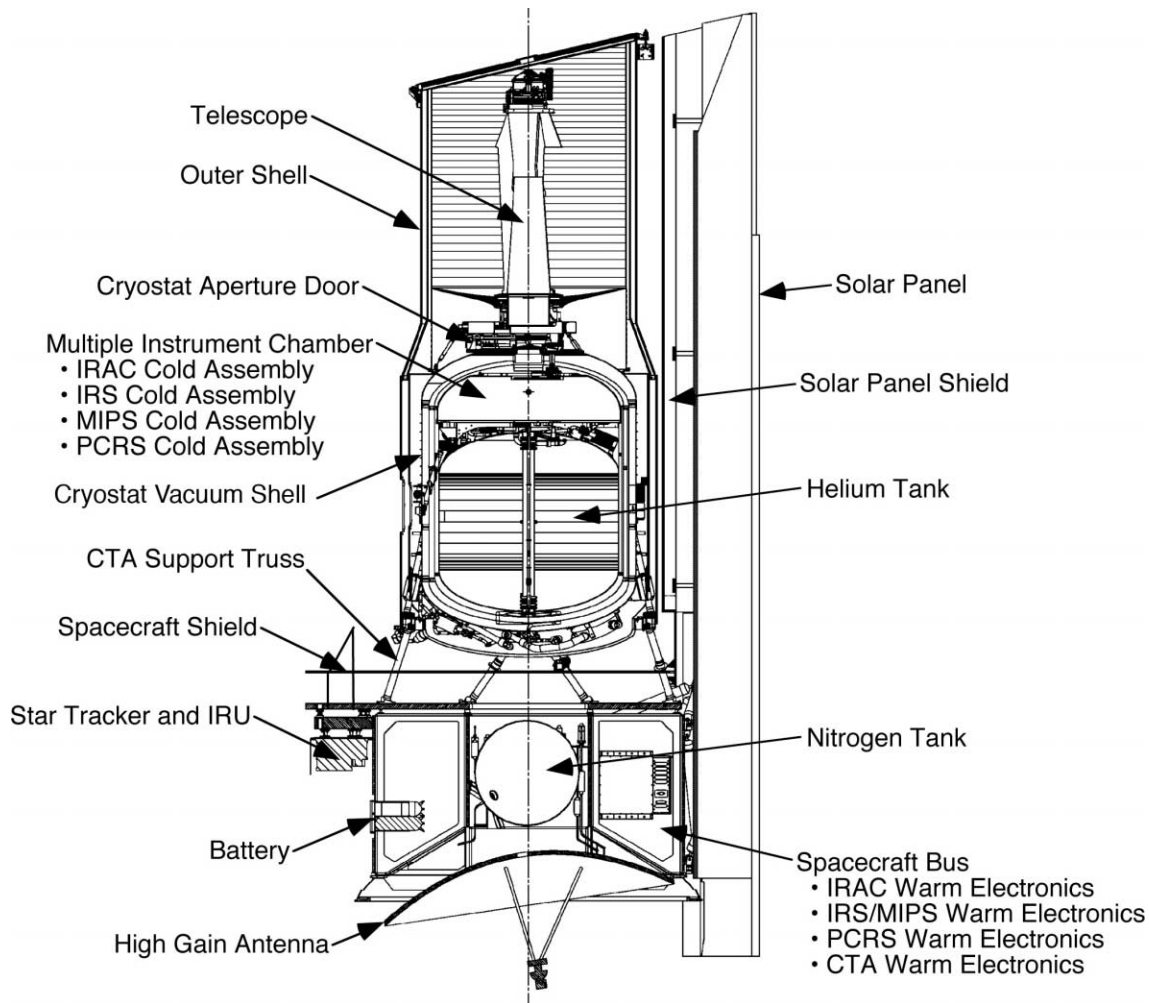


FIG. 1.—Cutaway view of the *Spitzer* flight hardware. The observatory is approximately 4.5 m high and 2.1 m in diameter. In this figure the dust cover is shown prior to its ejection approximately 5 days after launch.

The PCS comprises reaction wheels, gyroscopes, and star trackers. Four reaction wheels mounted in a pyramid arrangement provide redundancy against a single wheel failure. As the spacecraft is well outside the Earth's magnetic field, accumulated angular momentum is removed through an ambient-temperature, pressurized nitrogen gas RCS. The nitrogen gas plume does not affect the infrared environment or

the sensitive CTA thermal control surfaces. Twice a day a redundant pair of visible-light sensors (pointing calibration reference sensors [PCRS]) in the telescope focal plane provide calibration of the telescope boresight to the star trackers, which are mounted to the spacecraft structure.

The Cryogenic Telescope Assembly.—The CTA consists of the telescope assembly, the cryogenic portions of the three science instruments, a superfluid helium Dewar, and various thermal shields. *Spitzer* employs a novel thermal design (hereafter referred to as the “warm launch” design), in which most of the mass of the CTA, including the telescope and its baffles, is external to the cryostat vacuum shell and is launched at ambient temperature, only beginning to cool when on-orbit. This allows for a much smaller vacuum pressure vessel and a smaller total observatory mass than would a design based on the more conventional “cold launch” architecture used in the earlier *Infrared Astronomical Satellite (IRAS)* and *Infrared Space Observatory (ISO)* missions. The components of the CTA external to the cryostat are cooled after launch by a combination of radiation and helium boil-off vapor under a concept developed by F. Low and described in more detail in Lysek et al. (1995).¹³ A very low temperature CTA outer shell

TABLE 1
TOP-LEVEL OBSERVATORY PARAMETERS

Parameter	Value
Total Observatory mass at launch	861 kg
Dimensions (height × diameter).....	4.5 m × 2.1 m
Average operating power.....	375 W
Solar array generating capacity at launch	500 W
Nitrogen reaction control gas at launch	15.59 kg
Estimated reaction control gas lifetime.....	17 yr
Mass memory capacity	2 Gbytes
Telescope primary diameter.....	0.85 m
Telescope central obscuration.....	14.2%
Superfluid helium at launch.....	337 l
Estimated nominal cryogenic lifetime.....	5.3 yr
Data transmission rate (high-gain antenna up to 0.58 AU from Earth).....	2.2 Mb s ⁻¹
Command communication rate.....	2 kbps

¹³ Other possible applications of radiative cooling to the design of an infrared space observatory are described in Burnell et al. (1992), and alternate configurations were also proposed by H. Moseley at about the same time.

TABLE 2
INFRARED ARRAY CAMERA (IRAC): FOUR-CHANNEL INFRARED IMAGER

Channel	Wavelength (μm)	Field of View (arcmin)	Detector
1.....	3.19–3.94	5.2×5.2	256×256 InSb
2.....	4.00–5.02	5.2×5.2	256×256 InSb
3.....	4.98–6.41	5.2×5.2	256×256 Si:As
4.....	6.45–9.34	5.2×5.2	256×256 Si:As

NOTE.—PI: G. G. Fazio, Smithsonian Astrophysical Observatory; instrument built at NASA Goddard Space Flight Center.

is critical to the achievement of a long mission lifetime with a small cryostat, but requires excellent thermal isolation between warm and cold components as well as tight restrictions on the orientation of the flight hardware with respect to the Sun. The CTA outer shell is painted with high-emissivity black paint on the side that faces away from the Sun and is polished aluminum on the sides that face the thermal shields, solar array, and warm spacecraft components. The *Spitzer* warm launch design and the wide range of infrared wavelengths observed by the focal plane instruments require an open aperture in the vacuum cryostat after launch to allow the passage of infrared light from the telescope into the instrument chamber. For this purpose a removable vacuum window was constructed of gold-film-coated sapphire to allow the cold instruments to perform visible and near-infrared alignment of the CTA optical train on the ground without having to deploy the window prior to launch. A dust cover over the outer shell aperture that was ejected 4.9 days after launch, and 0.9 days prior to the opening of the cryostat window, was the only other deployable mechanism on the *Spitzer* observatory.

The telescope optics and metering structure are constructed entirely of beryllium, minimizing changes in both the telescope prescription and its alignment with the focal plane as the telescope cools on-orbit. A moveable secondary capable of motion only along the optical axis was installed to compensate for any changes in focus due to gravity release and uncertainties in the ground testing of the telescope. The telescope optics are not cooled directly by the helium bath but are thermally coupled to the cryostat vacuum shell, which is cooled by the superfluid helium boil-off vapor. The higher the boil-off rate, the colder the telescope. The telescope temperature necessary to keep thermal emission from the optics negligible compared to the natural zodiacal background decreases with wavelength, reaching 5.6 K for the 160 μm

channel in the Multiband Infrared Photometer for *Spitzer* (MIPS) instrument. MIPS itself does not dissipate enough power in its cold assemblies to provide the necessary boil-off rate for this temperature; a small adjustable heater in the cryogen provides a few extra milliwatts of power if needed. The helium liquid-gas interface is constrained within a porous plug phase separator, preventing rapid helium coolant loss.

3. INSTRUMENT PAYLOAD

Three infrared instruments, the Infrared Array Camera (IRAC), the Infrared Spectrograph (IRS), and the MIPS, share a common focal plane. Their fields of view are defined by pick-off mirrors, as shown in Figure 2 (Plate 1). The top level design and performance characteristics of the instruments are described in Tables 2–4. The instruments achieve great scientific power through the use of state-of-the-art infrared detector arrays in formats as large as 256×256 pixels. For broadband imaging and low spectral resolution spectroscopy, *Spitzer* has achieved sensitivities close to or at the levels established by the natural astrophysical backgrounds—principally the zodiacal light—encountered in Earth orbit (Fig. 3). The only moving part in use in the entire science instrument payload is a scan mirror in the MIPS. The instrument aperture is selected by body-pointing the entire observatory.

4. ORBIT

Spitzer utilizes a unique Earth-trailing solar orbit (as of 2004 March 26 *Spitzer* was trailing 0.083 AU behind the Earth). As seen from Earth, *Spitzer* recedes at about 0.12 AU yr^{-1} and will reach a distance of 0.62 AU in 5 years. The Earth-trailing orbit has several major advantages over a low Earth orbit for *Spitzer*. The principal advantage is being away from the heat of the Earth; this enables the warm-launch architecture and the extensive use of radiative cooling, which makes *Spitzer*'s cryothermal design extremely efficient. More precisely, the solar orbit allows the spacecraft always to be oriented with the solar array pointed at the Sun, while the black side of the outer shell has a complete hemispherical view of deep space with no interfering heat sources, enabling the radiative cooling of the outer shell described earlier. The absence of eclipses in the solar orbit makes for an extremely stable thermal configuration and reduces variability of the alignment between the cold telescope and the warm star tracker and inertial reference unit (gyroscopes) to less than 0.5 over timescales of days. Operationally, the orbit permits excellent sky viewing and observing efficiency (Kwok 1993). Finally, while in a solar orbit the observatory is not affected by

TABLE 3
INFRARED SPECTROGRAPH (IRS): LOW- TO MODERATE-RESOLUTION SPECTROMETER

Module	Wavelength Range (μm)	Slit Dimensions (arcsec)	Spectral Resolution $\lambda/\Delta\lambda$
Short-Low	5.2–7.7, second-order	3.6×57	80–128
	7.4–14.5, first-order	3.7×57	64–128
Long-Low.....	14.0–21.3, second-order	10.5×168	80–128
	19.5–38.0, first-order	10.7×168	64–128
Short-High.....	9.9–19.6	4.7×11.3	~600
Long-High.....	18.7–37.2	11.1×22.3	~600
Peak-up array (blue).....	13.3–18.7	56×80	3
Peak-up array (red).....	18.5–26.0	54×82	3

NOTE.—PI: J. R. Houck, Cornell University; instrument built at Ball Aerospace.

TABLE 4
MULTIBAND INFRARED PHOTOMETER FOR *Spitzer* (MIPS): FAR-INFRARED IMAGER
AND SPECTRAL ENERGY DISTRIBUTION (SED) PHOTOMETER

Band Identification	Wavelength Range (μm)	Field of View (arcmin)	Detector Array
24 μm	21.5–26.2	5.4 \times 5.4	128 \times 128 Si:As
70 μm	62.5–81.5	5.2 \times 5.2 ^a	32 \times 32 Ge:Ga
160 μm	139.5–174.5 ^b	5.3 \times 0.5	2 \times 20 Stressed Ge:Ga
SED ($\lambda/\Delta\lambda = 15\text{--}25$)	51–106	2.7 \times 0.34	32 \times 24 Ge:Ga

NOTE.—PI: G. H. Rieke, University of Arizona; instrument built at Ball Aerospace.

^a The MIPS 70 μm array consists of two 5'2 \times 2'6 halves. Because of a problem in the cold cabling, one of the halves has significantly worse sensitivity than the other.

^b The MIPS 160 μm channel has a short-wavelength filter leak that admits some 1.6 μm light that must be accounted for when observing blue objects. See the *Spitzer* Science Center Web site for more information.

the charged particles in the Van Allen radiation belts. These thermal and charged-particle advantages are shared by the L2 orbit contemplated for the *James Webb Space Telescope* (*JWST*). Unlike an L2 orbit, however, *Spitzer*'s heliocentric orbit eliminates the need for station-keeping, allowing the use of a smaller and less costly launch vehicle.

The orbit has two disadvantages. First, as *Spitzer* moves away from the Earth, the power margins for data transmission and command communication decrease, forcing changes in communication strategy and, eventually, somewhat reduced efficiency as more time is spent communicating with the ground stations. The data are transmitted to the antennae of the Deep Space Network by orienting the spacecraft so that a fixed X-band antenna located on the bottom of the spacecraft

is pointed at the Earth. Our current data transmission strategy of two \sim 45 minute passes per day at a data rate of 2.2 Mbps is robust for at least the first 2.5 yr of the mission. Second, outside of the protection of the Earth's magnetosphere *Spitzer* is more susceptible to solar proton storms and is subject to a higher quiescent Galactic cosmic ray flux. However, as mentioned above, *Spitzer* is also free from the daily passages through the South Atlantic Anomaly, which provide the main radiation dose in low Earth orbit.

During its in-orbit checkout period *Spitzer* encountered a very large solar proton storm beginning 2003 October 28. During the 2 day period of this storm the observatory received an integrated dose of $1.6 \times 10^9 p^+ \text{cm}^{-2}$ for proton energies greater than 50 MeV, roughly the integrated dose expected under normal conditions over the first 2.5 yr of operations. During the course of the storm the science instruments were powered off. Aside from a small number (<4%) of IRS detector pixels that exhibited increased dark current, a correctable change in the offset bias of the wide-angle sun sensors on the spacecraft, and a very slight decrease in the efficiency of its solar arrays, the observatory was unaffected by this event.

5. OPERATIONS

The users' operational interface to the observatory is through the *Spitzer* Science Center (SSC) at the California Institute of Technology, which is responsible for science program selection and scheduling, calibration, pipeline processing, and data distribution and archiving. The SSC collaborates with mission and spacecraft operations teams at the Jet Propulsion Laboratory and Lockheed Martin, Denver, in preparing and executing the on-orbit sequences.

The underlying principle of the science operations is that of the Astronomical Observational Template (AOT), a Web-based menu that the user fills in to define a particular observation. A completed AOT becomes an Astronomical Observational Request, or AOR.

The AOR created by the observer is expanded directly into a series of spacecraft commands, and the executed sequence consists of a series of AORs, each individually lasting between 10 minutes and 6 hr, interspersed with spacecraft activities such as pointing-system calibrations and data transmission.

Only one instrument operates at a time; there are no parallel observations or internal calibrations, greatly simplifying the on-board architecture and software. Because the helium use is dominated by the instrument cold-power dissipation, operating two instruments at once would halve the lifetime even as the instantaneous data rate doubled.

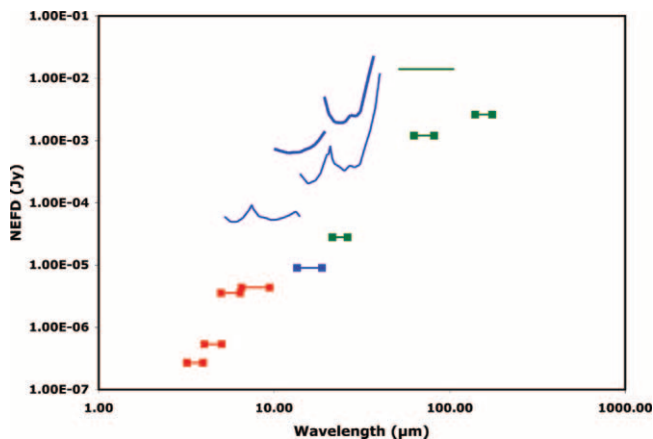


FIG. 3.—Point-source sensitivity and wavelength coverage of the *Spitzer* science instruments. All data are for 500 s integration times and are 1σ . In most cases the realized sensitivity can depend strongly on the zodiacal emission level, background confusion, and for the MIPS 70 μm array, which half of the array is being used. The data presented here are for the most optimal locations on the sky and the most sensitive half of the MIPS 70 μm array. The red lines with square endpoints show the IRAC sensitivity and wavelength coverage. The blue lines denote the IRS; the blue line with the square endpoints shows the IRS blue peak-up array when used for imaging. The IRS red peak-up array performance is not shown on this plot, as it is very similar to the MIPS 24 μm channel in its wavelength coverage, but is not as sensitive. The blue lines without endpoints show the IRS spectral coverage and sensitivity, with the thicker lines denoting the high-resolution modules and the thinner lines the low-resolution module. The green lines with endpoints show the MIPS sensitivity and wavelength coverage. The green line without endpoints shows the predicted MIPS SED performance, although since this operational mode has not been commissioned yet there is only incomplete flight data available on its sensitivity.

With the large fraction ($\sim 35\%$) of the sky that is accessible at any time, *Spitzer* can be operated with high efficiency. Our target is to achieve an on-orbit efficiency (defined as $1 - f_c$, where f_c is the fraction of wall-clock time spent in spacecraft calibration and data transmission) of 0.9. Prelaunch simulations suggested that the efficiency could exceed 0.88 on-orbit, and early results from the first few months of normal operations show that we should reach the 0.9 level as our operational experience accumulates.

6. OBSERVING TIME UTILIZATION

Observing time on *Spitzer* is divided among three major categories of users: General Observers (GO), Legacy Science Teams, and Guaranteed Time Observers (GTO). The GTOs receive 20% of the time for the first 2.5 yr and 15% thereafter. In addition, up to 5% of the observing time can be allocated as Director's Discretionary Time, while the balance of the time is available for GO use. Six Legacy Science teams were selected prior to launch to carry out large-scale projects with the joint objectives of creating a coherent scientific legacy and seeding the *Spitzer* archive with data that will stimulate follow-up proposals from the entire scientific community. Details of the currently planned GTO and Legacy programs can be found on the SSC Web site. The GO time constitutes $\sim 75\%$ of the available observing time; this is available to the worldwide scientific community through the usual peer-review process and will be allocated on an annual basis. GO Cycle 1 proposals were submitted in 2004 February, and Cycle 1 observations will begin in 2004 July. For the next cycle, with proposals due in 2005 February, ~ 5000 hr of GO observing time will be allocated.

7. ON-ORBIT STATUS

Spitzer requires the unique low thermal environment of space in order to function properly; the environment both permits the necessary radiative cooling and provides the low backgrounds to allow the science instruments to achieve their high sensitivities. This environment was difficult or impossible to simulate on the ground, so there was some uncertainty as to how well the observatory would perform in orbit. We are pleased to report that in almost every respect the on-orbit performance of the observatory meets or exceeds expectations. The on-orbit performance of the instruments is summarized above, and more details can be found in Fazio et al. (2004), Houck et al. (2004), and Rieke et al. (2004). Aside from the science instrument sensitivities, the most important on-orbit performance characteristics are listed below.

Thermal.—The outermost CTA shield (the “outer shell”) attained its final temperature of 34–34.5 K solely by radiative cooling, and the telescope cooled to its operating temperature of 5.6 K in 41 days. The mass of the helium remaining after the initial cool-down was measured to be 43.4 kg by applying a heat pulse to the helium bath 57 days after launch and measuring the accompanying temperature rise. To maintain the telescope at 5.5 K requires a total heat of 5.6 mW to the helium bath, leading to a boil-off of approximately 22 g of helium per day. For a fixed telescope temperature, these nominal numbers translate into a 5.3 yr postlaunch lifetime. In a worst-case scenario in which all of the engineering uncertainties stack against us, the lifetime would drop to 4.0 yr, which still compares quite favorably with the mission minimum lifetime requirement of 2.7 yr. By regulating the power dissipation to accommodate the telescope temperature requirements of the instrument that is in use, we are expecting

at least an additional 4 months of cryogenic lifetime beyond the nominal 5.3 yr. The only other expendable, the N_2 gas in the RCS system, should last for more than 10 yr. Following the depletion of the cryogenics, the telescope will warm up, but it will still be colder than the outer shell. Current estimates suggest that the telescope temperature will always be less than 30 K. At this temperature, both the instrumental background and the detector dark current should be low enough for *Spitzer* to continue natural background-limited operations in the shortest wavelength IRAC bands at 3.6 and 4.5 μm . Additional information on the measured on-orbit thermal performance of the *Spitzer* CTA can be found in Finley et al. (2004).

Optical performance, including focus.—A focus campaign of two secondary mirror movements was initiated once the telescope assembly had cooled to operating temperature to achieve the final focus (Hoffmann et al. 2004). On-orbit measurements of the telescope then showed that it provides diffraction-limited performance at wavelengths greater than 5.5 μm , which compares favorably with the requirement of 6.5 μm (Gehrz et al. 2004). After the completion of this campaign all of the science instruments were measured to be confocal to within the depths of their focus.

Pointing performance.—In general, the pointing performance of *Spitzer* is better than the nominal predictions. The star tracker has proven to be very accurate, with a noise-equivalent-angle of approximately $0''.11$ using an average of 35 tracked stars. The cryomechanical variation in alignment over time between the star tracker mounted on the warm spacecraft and the cold telescope boresight has proven to be very small and easily calibrated, so that the star tracker can be used to directly point the telescope boresight to better than $1''$, 1σ rms radial uncertainty. For offset movements less than $30'$, the PCS meets the $0''.4$ offset accuracy requirement. It takes less than 150 s for the telescope to slew 15° and to settle to its commanded position to within the above tolerances. Once the telescope pointing has settled, it is stable to within $0''.03$, 1σ rms radial uncertainty, for times up to 600 s. Observations of a number of solar system targets demonstrated that the PCS is able to track such objects at rates up to $0''.14\text{ s}^{-1}$. The PCS has also demonstrated smooth scanning during MIPS scanning observations at rates of $2''$, $6''$, and $20''\text{ s}^{-1}$.

External torques and reaction control.—Net angular momentum will build up on-orbit from a combination of solar pressure and uncompensated helium venting. During the design of the observatory, care was taken to align the vector of solar pressure with the center of mass as closely as possible, and the two CTA helium vent nozzles were also balanced very well. This has resulted in very low momentum build-up and infrequent—once or twice per week—actuators of the reaction control system to remove angular momentum.

8. SUMMARY AND CONCLUSIONS

The *Spitzer Space Telescope* has been operating at high efficiency since 2003 December. The early scientific results presented in this special volume, based largely on observations made prior to 2004 March, are indicative of *Spitzer's* great power and promise. We welcome the participation of the entire scientific community over the next 5 years in using this important new facility to expand yet further our understanding of the universe.

9. ACKNOWLEDGMENTS

The *Spitzer Space Telescope* is operated by the Jet Propulsion Laboratory, California Institute of Technology, under

NASA contract 1407. Support for this work was provided by NASA through an award issued by JPL/Caltech. T. Roellig would like to acknowledge the support of the NASA Office of Space Sciences.

The success of the *Spitzer Space Telescope* reflects the talent and dedication of thousands of people who have worked on this project over the past two decades and more. The authors of this paper consider it a privilege to recognize our colleagues who have contributed to this success. Here we list many of these people, by the institutions through which they participated in the definition, development, and/or early operations of *Spitzer*. We hope that this recognition provides a tangible though modest token of our gratitude and that they—and others whom we may have inadvertently omitted from the lists—are able to share with us the excitement of the first fruits of our collective labors.

Ball Aerospace (Cryogenic Telescope Assembly): R. Abbott, D. Adams, S. Adams, J. Austin, B. Bailey, H. Bareiss, J. Barnwell, T. Beck, B. Benedict, M. Bilkey, W. Blalock, M. Breth, R. Brown, D. Brunner, D. Burg, W. Burmester, S. Burns, M. Cannon, W. Cash, T. Castetter, M. Cawley, W. Cebula, D. Chaney, G. J. Chodil, C. Cliff, S. Conley, A. Cooper, J. Cornwell Sr., L. Cortelyou, J. Craner, K. Craven, D. Curtis, F. Davis, J. Davis, C. Dayton, M. Denaro, A. DiFronzo, T. Dilworth, N. Dobbins, C. Downey, A. Dreher, R. Drewlow, B. Dubrovin, J. Duncan, D. Durbin, S. Engles, P. Finley, J. Fleming, S. Forrest, R. Fredo, K. Gause, M. Gee, S. Ghesquiere, R. Gifford, J. Good, M. Hanna, D. Happs, F. Hausle, G. Helling, D. Herhager, B. Heurich, E. Hicks, M. Hindman, R. Hopkins, H. Hoshiko Jr., J. Houlton, J. Hueser, J. Hurt, W. Hyatt, K. Jackson, D. Johnson, G. Johnson, P. Johnson, T. Kelly, B. Kelsic, S. Kemper, R. Killmon, R. Knewton, T. Konetski, B. Kramer, R. Kramer, L. Krauze, T. Laing, R. LaPointe, J. Lee, D. Lemon, P. Lien, R. Lytle, L. Madayeu, M. Mann, R. Manning, J. Manriquez, M. Martella, G. Martinez, T. McClure, C. Meier, B. Messervy, K. Modafferi, S. Murray, J. Necas Jr., M. Neitenbach, P. Neuroth, S. Nieczkoski, G. Niswender, E. Norman-Gravseth, R. Oonk, L. Oystol, J. Pace, K. Parrish, A. Pearl Jr., R. Pederson, S. Phanekham, C. Priday, B. Queen, P. Quigley, S. Rearden, M. Reavis, M. Rice, M. Richardson, P. Robinson, C. Rowland, K. Russell, W. Schade, R. Schildgen, C. Schroeder, G. Schultz, R. Schweickart, J. Schweinsberg, J. Schwenker, S. Scott, W. Seelig, L. Seide, K. Shelley, T. Shelton, J. Shykula, J. Sietz, J. Simbai, L. Smeins, K. Sniff, B. Snyder, B. Spath, D. Sterling, N. Stoffer, B. Stone, M. Taylor, R. Taylor, D. Tennant, R. Tio, P. True II, A. Urbach, S. Vallejo, K. Van Leuwen, L. Vernon, S. Volz, V. VonRuden, D. Waldeck, J. Wassmer, B. Welch, A. Wells, J. Wells, T. Westgard, C. Williamson, E. Worner Jr., T. Yarnell, J. Yochum, A. Youmans, J. Zynsky.

Cornell University (Infrared Spectrograph): *Cornell (project management and science):* D. Barry, S. V. W. Beckwith, J. Bernhard-Salas, C. Blacken, V. Charmandaris, M. Colonna, S. Corbin, P. Devine, D. Devost, J. Diller, K. Duclos, E. Furlan, G. Gull, P. Hall, L. Hao, C. Henderson, T. Herter, J. Higdon, S. Higdon, P. Howell, L. McCall, A. Parks, B. Pirger, A. Rakowski, S. Reinehart, A. Reza, E. E. Salpeter, J. Schoenwald, G. Sloan, J. Smith, H. Spoon, K. Uchida, D. Weedman, J. Wilson; **University of Rochester:** D. M. Watson, W. F. Forrest; **California Institute of Technology:** K. Matthews; **Ball Aerospace (instrument development):** D. Alderman, D. Anthony, M. Bangert, J. Barnwell, A. Bartels, S. Becker, W. Belcher, J. Bergstrom, D. Bickel, M. Bolton, S. Burcar, D. Burg, S. Burns, S. Burns, D. Burr, P. Burrowes,

W. Cebula, C. Conger, J. Crispin, M. Dean, M. D'Ordine, S. Downey, R. Drewlow, L. Duchow, D. Eva, C. Evans, M. Foster, S. Fujita, D. Gallagher, A. Gaspers, P. Gentry, S. Giddens, J. Graw, M. Hanna, A. Haralson, M. Henderson, D. Herhager, J. Hill, S. Horacek, M. Huisjen, S. Hunter, J. Jacob, R. Karre, L. Larsen, P. Lien, R. Manning, J. Marriott, D. McConnell, R. McIntosh, M. McIntosh, G. Mead, B. Michelson, B. Miller, J. Moorehead, M. Morris, J. Murphy, M. Nelson, J. Pacha, I. Patrick, A. Pearl, B. Pett, S. Randall, C. Rowland, R. Sandoval, D. Sealman, K. Shelley, J. Simbai, L. Smeins, C. Stewart, G. Taudien, D. Tennant, J. Troeltzsch, B. Unruh, C. Varner, J. Winghart, J. Workman; **Rockwell (detector arrays):** B. Beardwood, J. Huffman, D. Reynolds, D. Seib, M. Stapelbroek, S. Stetson; **OCLI (filters):** S. Corda, B. Dungan, D. Favot, S. Highland, M. Inong, V. Jauregui, C. Kennemore, B. Langley, S. Mansour, R. Mapes, M. Mazzuchi, C. Piazza.

Jet Propulsion Laboratory, California Institute of Technology (project and science management, mission operations): D. Achhnani, A. Agrawal, T. Alfery, K. Anderson, J. Arnett, B. Arroyo, D. Avila, W. Barboza, M. Bareh, S. Barry, D. Bayard, C. Beichman, M. Beltran, R. Bennett, P. Beyer, K. Bilby, D. Bliss, G. Bonfiglio, M. Bothwell, J. Bottenfield, D. Boussalis, C. Boyles, M. Brown, P. Brugarolas, R. Bunker, C. Cagle, C. Carrion, J. Casani, E. Cherniack, E. Clark, D. Cole, J. Craft, J. Cruz, M. Deutsch, J. Dooley, S. Dekany, R. Dumas, M. Ebersole, C. Elachi, W. Ellery, D. Elliott, K. Erickson, J. Evans, J. Fanson, T. Feehan, R. Fragoso, L. Francis, M. Gallagher, G. Ganapathi, M. Garcia, T. Gavin, S. Giacoma, J. Gilbert, L. Gilliam, C. Glazer, P. Gluck, V. Gorjian, G. Greanias, C. Guernsey, A. Guerrero, M. Hashemi, G. Havens, C. Hidalgo, E. Higa, J. Hodder, H. Hotz, W. Hu, J. Hunt Jr., D. Hurley, J. Ibanez, K. Jin, M. Johansen, M. Jones, J. Kahr, B. Kang, P. Kaskiewicz, D. Kern, T. Kia, M. Kline, B. Korechoff, P. Kwan, J. Kwok, H. Kwong-Fu, M. Larson, M. Leeds, R. Lineaweaver, S. Linick, P. Lock, W. Lombard, S. Long, T. Luchik, J. Lumsden, M. Lysek, G. Macala, S. Macenka, N. Mainland, E. Martinez, M. Mcauley, J. Mehta, P. Menon, R. Miller, C. Miyamoto, W. Moore, F. Morales, R. Morris, A. Nakata, B. Naron, A. Nash, D. Nichols, M. Osmolovsky, K. Owen-Mankovich, K. Patel, S. Peer, N. Portugues, D. Potts, S. Ramsey, S. Rangel, R. Reid, J. Reimer, E. Rice, D. Rockey, E. Romana, C. Rondeau, A. Sanders, M. Sarrel, V. Scarffe, T. Scharton, H. Schember, C. Scott, P. K. Sharma, T. Shaw, D. Shebel, J. Short, C. Simon, B. Smith, R. Smith, P. Sorci, T. Specht, R. Spehalski, G. Squibb, S. Stanboli, K. Stapelfeldt, D. Stern, K. Stowers, J. Stultz, M. Tankenson, N. Thomas, R. Thomas, F. Tolivar, R. Torres, R. Tung, N. Vandermeij, P. Varghese, M. Vogt, V. Voskanian, B. Waggoner, L. Wainio, T. Weise, J. Weiss, K. Weld, R. Wilson, M. Winters, S. Wissler, G. Yankura, K. Yetter.

Lockheed-Martin (spacecraft, systems engineering, spacecraft operations): B. Adams, J. Akbarzadeh, K. Aline, T. Alt, G. Andersen, J. Arends, F. Arioli, A. Auyeung, D. Bell, R. Bell, F. Bennett, J. Bennett, M. Berning, H. Betts, M. Billian, S. Broadhead, B. Bocz, G. Bollendonk, N. Bossio, P. Boyle, T. Bridges, C. Brink, R. Brookner, J. Brunton, D. Bucher, M. Burrack, R. Caffrey, S. Carmer, P. Carney, T. Carpenter, R. Castro, J. Cattrysse, J. Cernac, G. Cesarone, K. Chan, C. Chang, M. Chuang, D. Chenette, A. Chopra, Z. Chou, W. Christensen, K. Chu, W. Clark, J. Clayton, S. Cleland, W. Clements, C. Colborn, A. Coopridge, B. Corwin, B. Costanzo, D. Cortes, M. Cox, M. Cox, J. Coyne, S. Curtin, G. Dankiewicz, C. Darr, J. Dates, J. Day, S. DeBrock, T. Decker, R. Defoe, J. Delavan, G. Delezynski, J. Delk, B. Dempsey,

R. Dodder, T. Dougherty, H. Drosdat, G. Du, B. Dudginski, M. Dunn, R. Dunn, M. Dunnam, D. Durant, D. Eckart, B. Edwards, M. Effertz, L. Ellis, P. Emig, N. Etling, M. Etz, N. Fernando, C. Figge, R. Finch, S. Finnell, A. Fisher, M. Fisher, P. Fleming, D. Ford, K. Foster, J. Frakes, P. Frankel, D. Fulton, P. Galli, D. Garcia, M. Gardner, B. Garner, S. Gaskin, S. Gasner, M. Geil, E. Georgieva, T. Gibson, B. Goddard, M. Gonzalez, D. Goold, D. Graves, S. Gray, I. Grimm, J. Grinwis, M. Gronet, R. Grubic, S. Guyer, M. Haggard, J. Harrison, G. Hauser, C. Hayashi, P. Headley, W. Hegarty, S. Heires, J. Herrerias, D. Hirsch, K. Hooper, J. Horwath, S. Housten, D. Howell, L. Huff, G. Idemoto, B. Jackson, K. Janeiro, K. Johnson, M. Johnson, R. Kaiser, P. Kallemeyn, G. Kang, R. Kasuda, M. Kawasaki, B. Keeney, J. Kenworthy, C. King, A. Klavins, K. Klein, C. Klien, P. Klier, C. Koch, L. Koch, D. Koide, R. Kriegbaum, J. Kuchera, J. Ladewig, D. Lance, M. Lang, K. Lauffer, A. Lee, E. Lee, J. Lee, R. Lee, D. Leister, K. Loar, A. Lott, C. Love, N. Iyengar, P. Ma, A. Magallanes, A. Mainzer, T. Maloney, S. Mar, B. Marquardt, M. Martin, G. Mason, R. Maxwell, R. May, G. McAllister, S. McElheny, M. McGee, J. McGowan, D. McKinney, A. McMechen, E. Merlo, C. Mifsud, J. Miles, S. Miller, A. Minter, C. Miran, S. Mittal, R. Mock, R. Mock, J. Montgomery, J. Moore, H. Mora, M. Moradia, L. Morales, R. Morales, G. Morison, J. Mota, F. Moules, S. Mumaw, L. Naes, A. Nalbandian, J. Nelson, L. Nenoff, J. Neuman, D. Nguyen, K. Nguyen, T. Nguyen, D. Niebur, D. Nishimura, M. Ochs, T. Oliver, J. Oo, J. Ortiz, G. Pace, L. Padgett, N. Page, G. Painter, H. Pandya, L. Pappas, N. Pemberton, R. Peterson, H. Phan, L. Phan, J. Pine, R. Poling, R. Potash, D. Radtke, W. Ramos, T. Ransom, M. Ratajczyk, D. Read, S. Ready, M. Rich, R. Richey, H. Rizvi, C. Rollin, C. Rudy, M. Rugebregt, R. Russek, B. Sable, C. Sandwick, M. Santos, N. Schieler, J. Schirle, G. Schlueter, M. Schmitzer, E. Sedivy, R. Seeders, S. Selover, R. Shaw, F. Sheetz, D. Shelton, R. Sherman, T. Sherrill, O. Short, R. Sison, B. Smith, F. Smith, S. Smith, B. Sotak, S. Spath, J. St. Pierre, K. Starnes, K. Stowers, J. Straetker, T. Stretch, S. Sulak, W. Sun, D. Swanson, C. Tatro, M. Tebo, D. Telford, A. Tessaro, J. Tietz, D. Tenerelli, J. Tolomeo, S. Toro-Allen, J. Tousseau, R. Traber, M. Tran, P. Travis, K. Uselman, S. Utke, N. Vadlamudi, R. VanBezooijen, J. Vantuno, R. Vasquez, G. Vergho, C. Voth, B. Vu, P. Wagner, M. White, M. Whitten, J. Wood, C. Worthley, D. Wright, C. Yanari, L. Yeaman, D. Zempel, S. Zeppa.

NASA Ames Research Center (project management through 1989): W. Brooks, P. Davis, A. Dinger, L. Manning, R. Melugin, J. Murphy, R. Ramos, C. Wiltsee, F. Witteborn, L. Young.

NASA Headquarters (program management): N. Boggess, L. Caroff, J. Frogel, F. Gillett, J. Hayes, W. Huntress, A. Kinney, L. LaPiana, K. Ledbetter, C. Pellerin, C. Scolise, H. Thronson, E. Weiler.

Smithsonian Astrophysical Observatory (Infrared Array Camera): SAO (project management and science): L. Allen, C. Arabadjis, M. Ashby, P. Barmby, V. Bawdekar, J. Boczenowski, D. Boyd, J. Campbell-Cameron, J. Chappell, M. Cohen, K. Daigle, L. Deutsch, L. Frazier, T. Gauron, J. Gomes, M. Horan, J. Huang, J. Huchra, E. Johnston, M. Kanouse, S. Kleiner, D. Koch, M. Marengo, S. Megeath, G. Melnick, W. Martell, P. Okun, M. Pahre, B. Patten, J. Polizzotti, J. Rosenberg, H. Smith, J. Spitzak, R. Taylor, E. Tollestrup, J. Wamback, Z. Wang, S. Willner; **NASA/ARC (Si:As detector array testing):** J. Estrada, R. Johnston, C. McCreight, M. McKelvey, R. McMurray, R. McHugh, N. Moss, W. Oglivie, N. Scott, S. Zins; **NASA/GSFC (instrument development):**

T. Ackerson, M. Alexander, C. Allen, R. Arendt, M. Armbruster, S. Babu, W. Barber, R. Barney, L. Bashar, C. Bearer, C. Bernabe, W. Blanco, R. Boyle, K. Breneman, G. Brown, M. Brown, G. Cammarata, S. Casey, P. Chen, M. Cushman, P. Davila, M. Davis, M. Dipirro, C. Doria-Warner, W. Eichhorn, D. Evans, D. Fixsen, J. Florez, J. Geiger, D. Gezari, D. Glenar, J. Golden, P. Gorog, S. Graham, C. Hakun, P. Haney, T. Hegerty, M. Jhabvala, F. Jones-Selden, R. Jungo, G. Karpati, R. Katz, R. Kichak, R. Koehler, R. Kolecki, D. Krebs, A. Kutuyev, J. Lander, M. Lander, N. Lee, J. Lohr, P. Losch, J. MacLoed, R. Maichle, S. Mann, N. Martin, P. Maymon, D. McComas, J. McDonnell, D. McHugh, J. Mills, C. Moiser, S. Moseley, T. Nguyen, T. Powers, K. Rehm, G. Reinhardt, J. Rivera, F. D. Robinson, C. Romano, M. Ryschkewitsch, S. Schwinger, K. Shakoorzadeh, P. Shu, N. Shukla, S. Smith, R. Stavely, W. Tallant, V. Torres, C. Trout, C. Trujillo, D. Vavra, G. Voellmer, V. Weyers, R. Whitley, J. Wolfgang, L. Workman, D. Yoder; **Raytheon Vision Systems (detector arrays):** C. Anderson, J. Asbrock, V. Bowman, G. Chapman, E. Corrales, G. Domingo, A. Estrada, B. Fletcher, A. Hoffman, L. Lum, N. Lum, S. Morales, O. Moreno, H. Mosel-Riedo, J. Rosbeck, K. Scharzt, M. Smith, S. Solomon, K. Sparkman, P. Villa, S. Woolaway; **University of Arizona:** T. Tysen, P. Woida; **University of Rochester (InSb detector array testing):** C. Bacon, R. Benson, H. Chen, J. Comparetta, N. Cowen, M. Drennan, W. Forrest, J. Garnett, B. Goss, S. Libonate, R. Madson, B. Marazus, K. McFadden, C. McMurtry, D. Myers, Z. Ninkov, R. Overbeck, J. Pipher, R. Sarkis, J. Schoenwald, B. White, J. Wu.

Spitzer Science Center, California Institute of Technology (science operations): W. Amaya, L. Amy, P. Appleton, L. Armus, J. Aronsson, D. Avila, S. Barba, R. Beck, C. Bennett, J. Bennett, B. Bhattacharya, M. Bica, C. Bluehawk, C. Boyles, H. Brandenburg, I. Bregman, J. Bruher, M. Burgdorf, S. Carey, J. Chavez, S. Comeau, D. Daou, A. Dean, M. Dobard, S. Dodd, R. Ebert, D. Fadda, S. Fajardo-Acosta, F. Fang, J. Fowler, D. Frayer, L. Garcia, W. Glaccum, T. Goldina, W. Green, C. Grillmair, E. Ha, E. Hacopians, T. Handley, R. Hartley, H. Heinrichsen, S. Hemple, D. Henderson, L. Hermans, T. Hesselroth, N. Hoac, D. Hoard, H. Hu, H. Hurt, H. Huynh, M. Im, J. Ingalls, E. Jackson, J. Jacobson, G. Johnson-McGee, K. Keller, A. Kelly, E. Kennedy, I. Khan, D. Kirkpatrick, S. Kolhatkar, M. Lacy, R. Laher, S. Laine, J. Lampley, W. Latter, W. Lee, M. Legassie, D. Levine, J. Li, P. Lowrance, N. Lu, J. Ma, W. Mahoney, D. Makovoz, V. Mannings, F. Marleau, T. Marston, F. Masci, H. McCallon, B. McCollum, D. McElroy, M. McElveny, V. Meadows, Y. Mei, S. Milanian, D. Mittman, A. Molloy, P. Morris, M. Moshir, R. Narron, B. Nelson, R. Newman, A. Noriega-Crespo, J. O'Linger, D. Padgett, P. Patterson, A. Pearl, M. Pesenson, S. Potts, W. Reach, L. Rebull, J. Rector, J. Rho, W. Roby, E. Ryan, R. Scholey, D. Shupe, N. Silbermann, G. Squires, S. Stolovy, L. Storrie-Lombardi, J. Surace, H. Teplitz, M. Thaller, G. Turek, S. Tyler, S. Van Dyk, S. Wachter, C. Waterson, W. Wheaton, J. White, A. Wiercigroch, G. Wilson, X. Wu, L. Yan.

University of Arizona (Multiband Imaging Photometer for Spitzer): Arizona (project management, array construction, and science): A. Alonso-Herrero, M. Alwardi, I. Barg, M. Blaylock, M. Bradley, M. Buglewicz, J. Cadien, A. Churchill, H. Dang, L. Davidson, J. T. Davis, H. Dole, E. Egami, C. Engelbracht, K. A. Ennico, J. Facio, J. Flores, K. D. Gordon, L. Hammond, D. Hines, J. Hinz, R. Hodge, T. Horne, P. Hubbard, D. M. Kelly, D. Knight, K. A. Kormos, E. LeFloc'h, F. J. Low, M. McCormick, T. J. McMahan, T.

Milner, K. Misselt, J. Morrison, K. Morse, J. Muzerolle, G. X. Neugebauer, L. Norvelle, C. Papovich, P. Perez-Gonzalez, M. J. Rieke, G. Rivlis, P. Rogers, R. Schnurr, M. Scutero, C. Siqueiros, P. Smith, J. A. Stansberry, P. Strittmatter, K. Su, C. Thompson, P. van Buren, S. Warner, K. White, D. A. Wilson, G. S. Winters; **University of California Berkeley/LBNL (science and detector material)**: E. Arens, J. W. Beeman, E. E. Haller, P. L. Richards; **Jet Propulsion Laboratory (science)**: C. Beichman, K. Stapelfeldt; **National Optical Astronomy Observatories (science)**: J. Mould; **Center for Astrophysics (science)**: C. Lada; **Ball Aerospace (instrument development)**: D. Bean, M. Belton, T. Bunting, W. Burmester, S. Castro, C. Conger, L. Derouin, C. Downey, B. Frank,

H. Garner, P. Gentry, T. Glenn, M. Hegge, G. B. Heim, M. L. Henderson, F. Lawson, K. MacFeely, B. McGilvray, R. Manning, D. Michika, C. D. Miller, D. Morgan, M. Neitenbach, R. Novaria, R. Ordonez, R. J. Pearson, Bruce Pett, K. Rogers, J. P. Schwenker, K. Shelley, S. Siewert, D. W. Strecker, S. Tennant, J. Troeltzsch, B. Unruh, R. M. Warden, J. Wedlake, N. Werholz, J. Winghart, R. Woodruff, C. Yanoski; **Raytheon (readout development)**: J. Asbrock, A. Hoffmann, N. Lum; **Ames Research Center (readout development)**: C. McCreight; **QM Industries (far-infrared filters)**: P. A. R. Ade; **Blackforest Engineering (engineering support)**: S. Gaalema; **Battell Engineering (engineering support)**: S. Battel; **SRON (scan mirror development)**: T. Degraauw.

REFERENCES

- Burnell, S. J. B., Davies, J. K., & Stobie, R. S. 1992, Next Generation Infrared Space Observatory (Dordrecht: Kluwer)
- Fazio, G. G., et al. 2004, ApJS, 154, 10
- Finley, P. T., Hopkins, R. A., & Schweickart, R. B. 2004, Proc. SPIE, 5487, 2
- Gehr, R. D., et al. 2004, Proc. SPIE, 5487, 86
- Hoffmann, W. F., Hora, J. L., Mentzell, J. E., Marx, C. T., Eisenhardt, P. R., Carey, S. J., & Megeath, S. T. 2004, Proc. SPIE, 5487, 88
- Houck, J. R., et al. 2004, ApJS, 154, 18
- Kwok, J. H. 1993, in AAS/AIAA Astrodynamics Conference, Aug. 16–19, 1993, ed. V. J. Modi et al. (Adv. Astronaut. Sci. 85; San Diego: Univelt/AAS), 1401
- Lysek, M. J., Israelsson, U. E., Garcia, R. D., & Luchik, T. S. 1995, in Advances in Cryogenic Engineering, Vol. 41, ed. P. Kittel (New York: Plenum), 1143
- Rieke, G., et al. 2004, ApJS, 154, 25

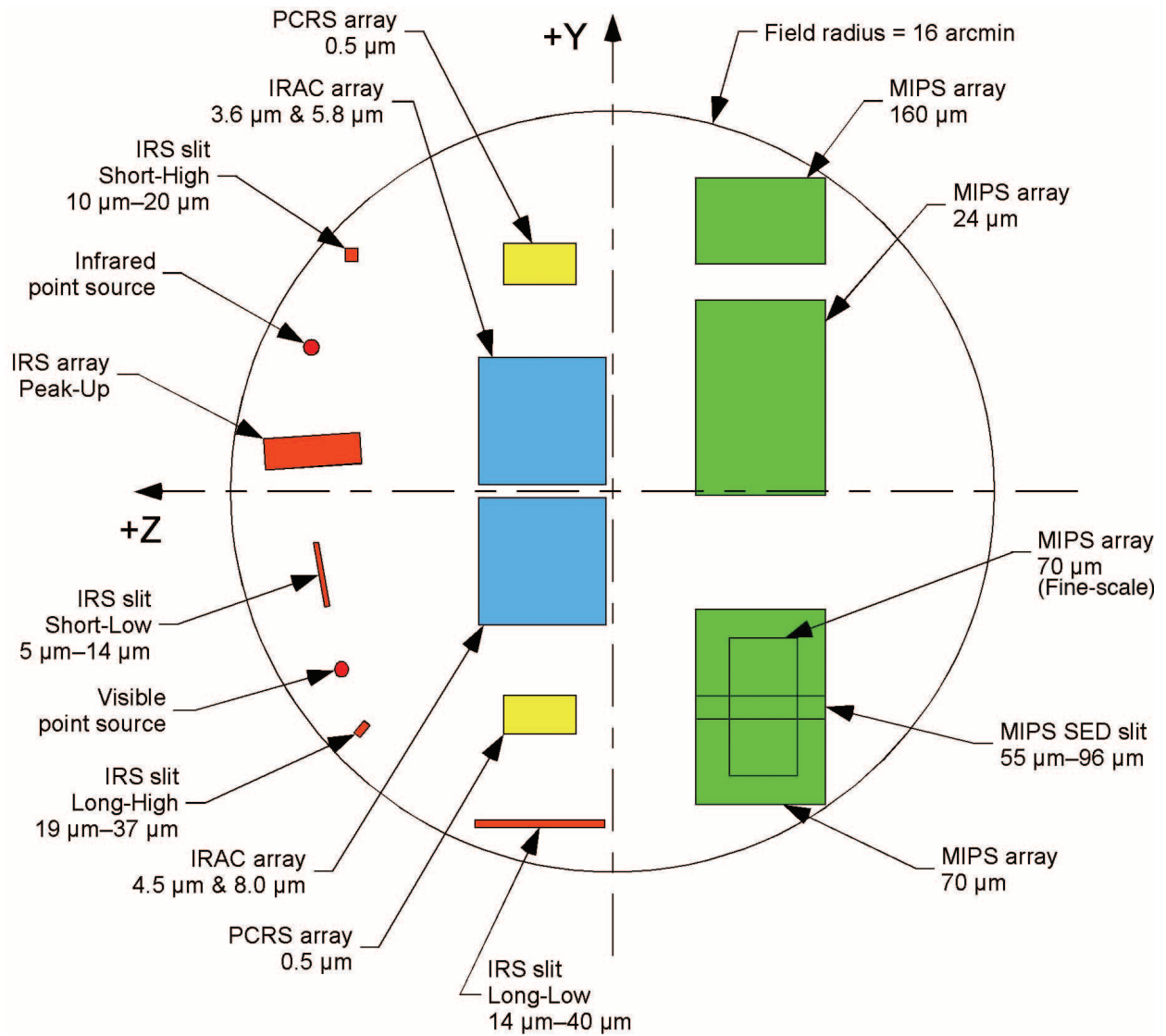


FIG. 2.—*Spitzer* focal plane layout as seen looking down from the telescope aperture. In this coordinate system the +Z direction points toward the sun. In addition to the science instrument apertures, the figure shows the location of the two pointing calibration reference sensor (PCRS) arrays and the two point sources that were used for ground-based focus checks and focal plane mapping. The MIPS apertures appear rectangular because the scan mirror accesses an area larger than the instantaneous footprint of the array; the position of the SED slit and the fine-scale array are shown schematically.